

Vibration Analysis of Rectangular Solid Plates and Plates with Surface Cracks

Venkat

Microwave Tube Research and Development Centre
DRDO, Bangalore, India

Dr. S.Ranganatha

Mechanical department
University Visvesvaraya College of Engineering
Bangalore University, Bangalore, India

Abstract— Plate members are used in automobile and aerospace structures. These structures are subjected to dynamic forces with variable frequencies due to engines used for propelling. These variable frequencies of dynamic forces cause resonance of plate elements in the structure. The resonance phenomenon leads to the fatigue of plate structures thus the instability of the flight in space.

In the present investigation an attempt has been made to characterize dynamic response, which controls the fatigue phenomenon of rectangular plates and plate with surface cracks oriented in different directions. The clamped-clamped-free-free (CCFF) boundary condition is incorporated. The vibration shaker is used to introduce exciting forces. The frequency of the exciting force is varied from 20 Hz to 2000 Hz. The amplitude, modal frequency, phase angle and damping factor are monitored at various resonant frequencies.

It is found from the experimental results that, amplitude of vibration, modal frequency, phase angle and damping factor are dependent on surface crack with longitudinal axis and its orientations.

Keywords— Surface crack, modal frequency, amplitude, damping factor, phase, vibration.

I.

INTRODUCTION

An aerospace and automobiles engineering industry utilize a system in which major sub components are plate structured elements. More specifically in aerospace, plate panels are used to a large extent. These plate elements are subjected to different frequencies and of varying range due to high speeds of aero engines. The large range of variable speeds of aero engines introduces forced excitation on plate panels. The plate experience response at specific frequencies called modal frequencies. The modal frequencies at higher modes in engineering structure, results in fatigue failure of the components.

Both experimental and numerical attempts are made by researchers to understand the dynamic response of plate structure.

Ivo Senjanovic made an attempt for estimating the natural frequency of free thin rectangular plate based on Rayleigh quotient method. The analytical estimated natural frequencies are compared with numerical obtained natural frequencies (1). Viswas and Ranjith studied both analytically and numerically methods to characterize free vibration of plates. Parameters like boundary conditions and plate thickness were considered for characterizing the dynamic response of the plate. The experimental method results were compared with results of numerical methods (2). Ibearugbulem and Owus studied the dynamic response of plate using energy method. The natural

frequency was obtained by using Taylor's series shape function and Ritz energy method. The results were compared with experimental work (3). Ilook Park and Usik lee studied dynamic response of plate using frequency dynamic spectral elements modeling and analysis method. The results were compared with exact solutions and numerical solutions (4). Khiem and Lien made an attempt in obtaining natural frequencies of beam with arbitrary number of cracks. The new method analyzed the effect of crack and boundary condition on natural frequencies (5). Zarza and Naimi made an attempt dynamic characteristic of isotropic and orthotropic cracked plate using energy approach. The results were comparable with numerical methods (6). Asif Israr et al., attempted a analytical modeling vibration analysis of partially cracked plate with different boundary condition. The method of multiple scales an approximate method was applied for solving the problem of cracked plate. The results were analyzed for both cracked length and plate thickness (7). Gharaibeh and Obeidat studied analytically the dynamic response of the rectangular plates. Rayleigh-Ritz method was used to calculate the first natural frequency. They used the results to characterize dynamic response in the presence of extra masses on the rectangular plates (8). Joshi et al., made analytical an attempt in characterizing, the dynamic response of internally cracked rectangular plate. They found that natural frequencies are more affected when cracks are internal and symmetrical about the mid plate of the plate. The influence was found that orientation of cracks with respect to longer edge of the crack was found to be more effective (9). Tushar choudary and Kumar made analytical attempts in predicting dynamic response of plate with circular hole. The results show that the natural frequency of the plates decreased with increased hole diameter (10). Ali and Atwal made analytical attempts to characterize the dynamic response of the rectangular plates with rectangular cut outs. They used the Rayleigh-Ritz method for finding the natural frequency. The results were compared with numerical methods (11). Ramamurthy et al., made attempts experimental attempt to find damping ratio. Such found damping ratio was used in numerical analysis (12). Maruyama and Ichinomiya conducted experiment for characterizing the dynamic response of clamped rectangular plates with straight narrow slits. Real time technique of the average interferometry was used to find the natural frequencies and mode shapes. The effect of the length of slit, position and inclination angle of slit on dynamic response was evaluated. They found that the above said parameters alter the dynamic response (13). Yin and lam developed analytical method for characterizing dynamic response of rectangular plates with two parallel cracks. The energy method was used for calculating natural frequencies

and also concluded that time domain response of the plate can be calculated using mode super position method (14). Gade and Khatode made analytical attempts for predicting dynamic response of beams with open edge crack. Parameters like varying crack, depth and location of the cracks were incorporated and studied the dynamic response of the beam. The result showed that the above parameter affects the dynamic response of the beam (15).

II. EXPERIMENTAL SETUP

The experiments are conducted using a 4-channel vibration controller, vibration shaker with accelerometer. The schematic experimental setup is shown Fig. 1.

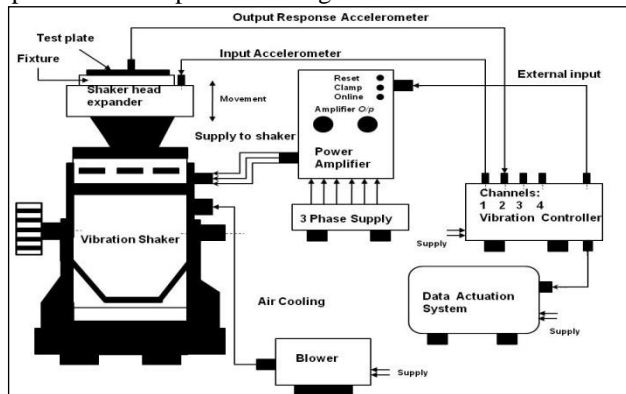


Fig. 1. Schematic of electrodynamic vibration set up

The details of the equipment/instruments used are shown in Table I. The solid rectangular plate and plate with surface cracks are shown in Fig. 2. The fixture used for obtaining clamped-clamped-free-free boundary condition is shown in Fig. 4 and Fig. 5.

TABLE I. SPECIFICATION OF SHAKER AND SUBSYSTEM

Subsystem	Model number	Parameter	Specification
Electro dynamic Shaker	SEV 060	Rated force	600 Kgf (Peak Sine)
Digital power amplifier	DAS 3K6	Operating frequency	5 Hz to 3000 Hz
Vibration controller	Spandon	Stroke	30 mm (p-p)
Piezo electric accelerometers	M353B04 (2 no's)	Acceleration bare table	75 g
RSTD package		Maximum velocity	1.5 m/sec
		Moving platform diameter	180 mm

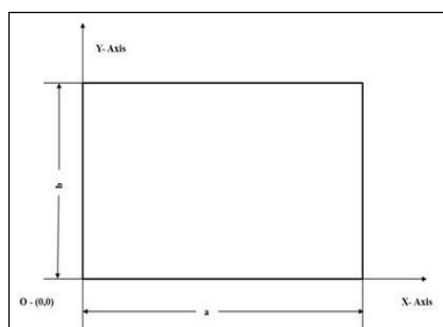


Fig. 2. Solid plate

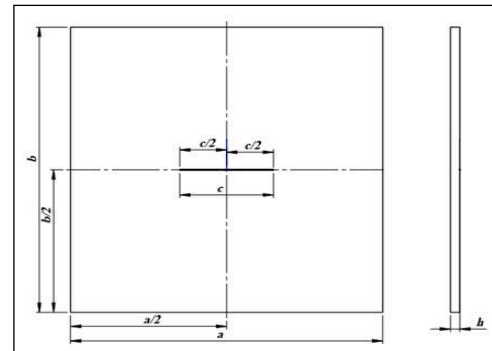


Fig. 3. Surface crack at 0° with longitudinal axis

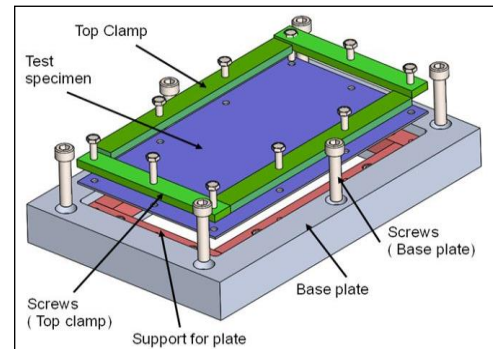


Fig. 4. Assembly fixture with specimen

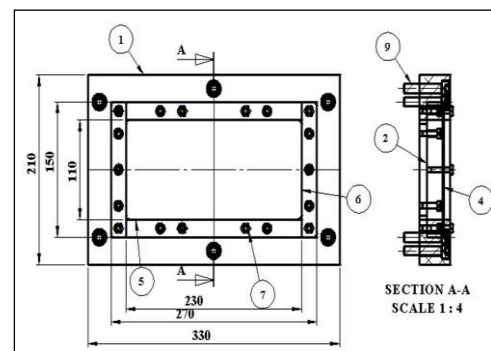


Fig. 5. 2 D drawing of vibration fixture

Fig. 6.



Fig. 7. Vibration shaker with plates for CCF boundary condition

The experiments are conducted with different orientation direction of the surface cracks. The different orientations of the crack with longitudinal axis used in experiments are

1. Solid plate
2. Surface crack at 0^0 with longitudinal axis
3. Surface crack at 20^0 with longitudinal axis
4. Surface crack at 40^0 with longitudinal axis
5. Surface crack at 60^0 with longitudinal axis
6. Surface crack at 80^0 with longitudinal axis
7. Surface crack at 90^0 with longitudinal axis

III. RESULTS AND DISCUSSION

A. Solid plate

Rectangular plate with clamped-clamped-free-free (CCFF) boundary condition was subjected to forced vibration. The experiment was repeated for three times and average values of parameters; modal frequency, amplitude, phase angle and damping factor were estimated. A typical plot of experimental results is shown in Fig. 8.

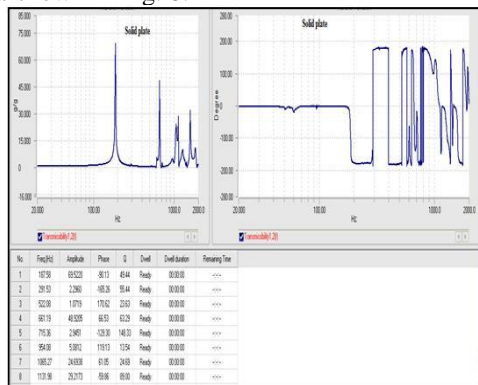


Fig. 8. Experimental results for solid plate for CCFF condition

The Fig. 8 shows different magnitude of amplitude, modal frequencies and phase angle at resonance. All the details regarding resonance frequencies, amplitude at resonance, phase angle and Q-factor s are also shown in Fig. 8. These data are used for drawing Fig. 9 which shows detailed information inclusively dependence of amplitude with exciting frequency.

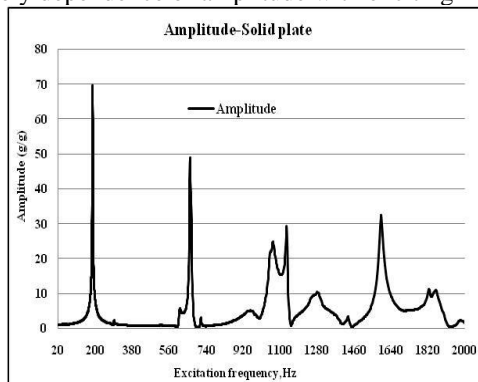


Fig. 9. Dependency of amplitude with excitation frequency for solid plate

The data of phase angle dependency on excitation frequencies are extracted from the Fig. 8 and drawn a new figure shown in Fig. 10 for the detailed information on phase angle of vibration.

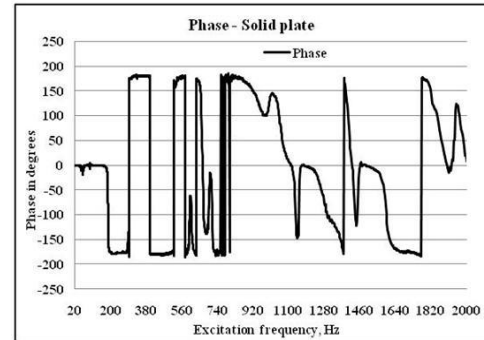


Fig. 10. Dependency of phase angles with modal frequency for solid plate

The experimental data in Fig. 8 are rounded off to nearest number. The amplitude is rounded up to full number, phase angle rounded up to full number. The frequencies are rounded up to full number and Q-factor rounded up to full number. The rounded off data of frequencies, amplitudes, phase angles and Q-factors are tabulated and shown in Table II. The damping factor (ξ) was found from the tabulated Q-factor values in the Table II. The damping factor (ξ) was estimated using formula: $\xi=1/2Q$ the estimated damping factors (ξ) are tabulated in Error! Reference source not found..

TABLE II. AMPLITUDE, MODAL FREQUENCY, PHASE, Q-FACTOR AND DAMPING FACTOR FOR SOLD PLATE

Solid plate					
Mode No.	Amplitude (g/g)	Modal Frequency (Hz)	Phase angle (0)	Q-Factor	Damping factor (ξ)
1	70	188	-90	49	0.02
2	2	292	-165	55	0.02
3	1	522	171	24	0.04
4	49	661	67	63	0.02
5	3	715	-129	148	0.01
6	5	954	119	14	0.07
7	25	1065	61	25	0.04
8	30	1132	-60	89	0.01

B. Surface crack at 0^0 with longitudinal axis

A typical plot of experimental results is shown in Fig. 11.

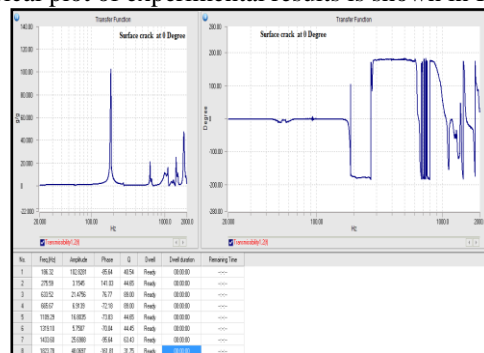


Fig. 11. : Experimental results for surface crack at 0^0 for CCFF conditions

The Fig. 11 shows different magnitude of amplitude, modal frequencies and phase angle at resonance. All the details regarding resonance frequencies, amplitude at resonance, phase angle and Q-factor are also tabulated in Fig. 11.

The data of amplitude dependency on excitation frequencies are extracted from the Fig. 11. These data is used for drawing Fig. 11 which shows information inclusively on dependency of amplitude with exciting frequency.

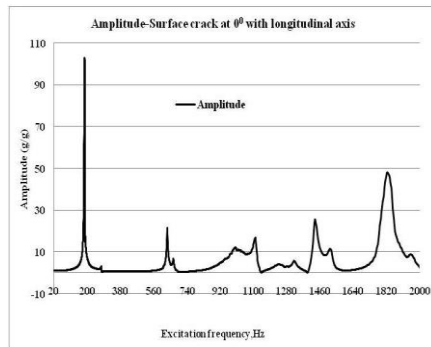


Fig. 12. : Dependency of amplitude with excitation frequency for surface crack at 0^0

The data of phase angle dependency on excitation frequencies are extracted from the Fig. 11 and drawn a new figure shown in Fig. 13 for the detailed information on phase angle of vibration.

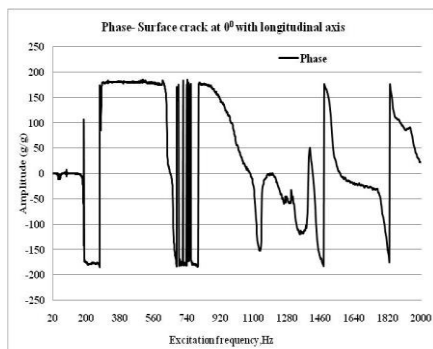


Fig. 13. Dependency of phase angles with excitation frequency for surface crack at 0^0

The experimental data of table in Fig. 11 are rounded off to nearest number. The amplitude is rounded up to first number, phase angle rounded up to full number. The frequencies are rounded up to full number and Q-factor rounded up to full number. The rounded off data of frequencies, amplitudes, phase and Q-factors are tabulated and shown in **Error! Reference source not found..** The damping factor (ξ) was found from the tabulated Q-factor values in the **Error! Reference source not found..** The damping factor (ξ) was estimated using formula: $\xi = 1/2Q$. The estimated damping factors (ξ) are tabulated in **Error! Reference source not found..**

TABLE III. AMPLITUDE, MODAL FREQUENCY, PHASE AND Q-FACTOR FOR SURFACE CRACK AT 0^0

Surface crack at 0^0 with longitudinal axis					
Mode No.	Amplitude (g/g)	Modal Freq.(Hz)	Phase (0)	Q-Factor	Damping Factor (ξ)
1	103	186	-86	41	0.01
2	3	276	141	45	0.01
3	22	634	77	89	0.01
4	7	666	-72	89	0.01
5	17	1109	-74	45	0.01
6	6	1319	-70	44	0.01
7	26	1434	-96	63	0.01
8	48	1824	-162	32	0.02

The **Error! Reference source not found.** shows the highest magnitude of amplitude 70g/g at resonance frequency was found in first mode which is 188 Hz. Other lesser magnitude of amplitude was found 49, 25 and 30 g/g at the resonance frequencies of 661, 1065 and 1132 Hz in mode 4, 7 and 8 respectively. The other minimum magnitude of

amplitude were found 2, 1, 3 and 5 g/g at the resonance frequencies 292, 522, 715 and 954 Hz in modes 2, 3, 5 and 6 respectively.

The **Error! Reference source not found.** shows highest magnitude of amplitude 103g/g at resonance frequency was found in first mode which is 186 Hz. Other lesser magnitude of amplitude was found 22, 17, 26 and 48 g/g at the resonance frequencies of 634, 1109, 1434 and 1824 Hz in mode 3, 5, 7 and 8 respectively. The other minimum magnitude of amplitude was found 3.2, 6.9 and 5.8g/g at the resonance frequencies 276, 666 and 1319 Hz in modes 2, 4 and 6 respectively.

The **Error! Reference source not found.** shows the phase angles at the resonance modes. The phase angles at the resonance modes were found to be 141 and 77^0 at the modes 2 and 3 respectively. The response during these modes is lagging to forcing disturbance. The lagging found to be maximum in mode 2 and minimum in mode 2. The mode angles were found to be -86, -72, -74, -70, -96 and -162^0 at the modes 1, 4, 5, 6, 7 and 8 respectively. The response of the system during negative phase angle represents the leading of the system with respect to disturbing force. The leading was found to be highest in mode 8 and leading of the system gets reduced in modes 1, 4, 5, 6 and 7

The **Error! Reference source not found.** shows damping factor (ξ) varies from 0.01 to 0.02. The maximum damping factor was found 0.02 in mode 8 and minimum damping factor 0.01 were found in mode 1 to 8.

C. Surface crack at 20^0 with longitudinal axis

A typical plot of experimental results is shown in Fig. 14

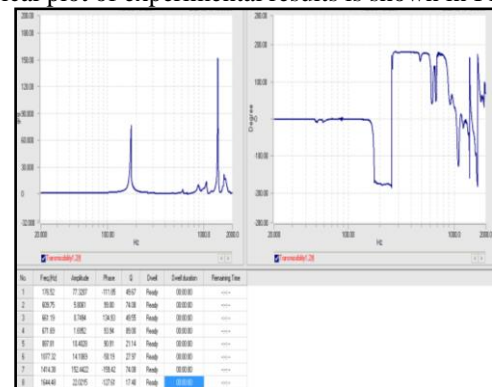


Fig. 14. : Experimental results for surface crack at 20^0 for CCFF conditions

The Fig. 14 shows different magnitude of amplitude, modal frequencies and phase angle at resonance. All the details regarding resonance frequencies, amplitude at resonance, phase angle and Q-factor are also tabulated in Fig. 14. The data of amplitude dependency on excitation frequencies are extracted from the Fig. 14. These data is used for drawing Fig. 15 which shows information inclusively on dependency of Amplitude with exciting frequency.

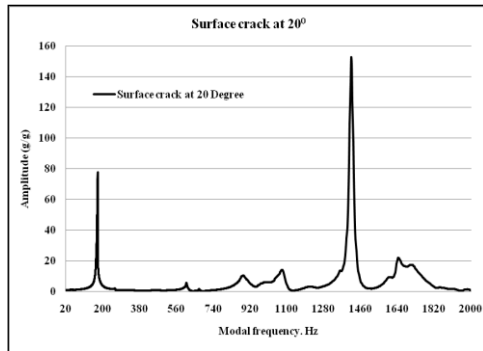


Fig. 15. Dependency of amplitude with excitation frequency for surface crack at 20°

The data of phase angle dependency on excitation frequencies are extracted from the Fig. 14 drawn a new figure shown in Fig. 16 for the detailed information on phase angle of vibration

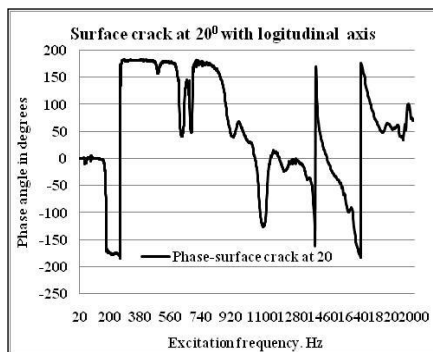


Fig. 16. Dependency of phase with excitation frequency for surface crack at 20°

The experimental data of table in Fig. 14 are rounded off to nearest number. The amplitude is rounded up to first digit, phase angle rounded up to full number. The frequencies are rounded up to full number and Q-factor rounded up to full number. The rounded off data of frequencies, amplitudes, phase and Q-factors are tabulated and shown in **Error! Reference source not found.**. The damping factor (ξ) was estimated using formula: $\xi = 1/2Q$. The estimated damping factors (ξ) are tabulated in **Error! Reference source not found.**

TABLE IV. AMPLITUDE, MODAL FREQUENCY, PHASE AND Q-FACTOR FOR SURFACE CRACK AT 20°

Surface crack at 20° with longitudinal axis					
Mode No.	Amplitude (g/g)	Modal Freq.(Hz)	Phase (°)	Q-Factor	Damping factor (ξ)
1	77	177	-112	50	0.01
2	6	610	99	74	0.01
3	1	661	135	50	0.01
4	2	672	94	89	0.01
5	10	888	91	21	0.02
6	14	1077	-50	28	0.02
7	152	1414	-159	74	0.01
8	22	1644	-128	17	0.03

The **Error! Reference source not found.** highest magnitude of amplitude 77g/g at resonance frequency was found in first and magnitude of 152g/g at resonance frequency was found in seventh mode which is 1414 Hz. Other lesser magnitude of amplitude was found 6, 10, 14 and 22 g/g at the

resonance frequencies of 610, 888, 1077 and 1644 Hz in mode 2, 5, 6 and 8 respectively. The other minimum magnitude of amplitude was found 01 and 2g/g at the resonance frequencies 661 and 672 Hz in modes 3 and 4 respectively.

The **Error! Reference source not found.** shows the phase angles at the resonance modes. The phase angles at the resonance modes were found to be 99, 135, 94 and 91° at the modes 2, 3, 4 and 5 respectively. The response during these modes is lagging to forcing disturbance. The lagging found to be maximum in mode 3 and minimum in mode 5. The mode angles were found to be -112, -50, -159 and -128° at the modes 1, 6, 7 and 8 respectively. The response of the system during negative phase angle represents the leading of the system with respect to disturbing force. The leading was found to be highest in mode 7 and leading of the system gets reduced in modes 1, 4, 5, 6 and 8.

The **Error! Reference source not found.** shows damping factor (ξ) varies from 0.01 to 0.03. The maximum damping factor was found 0.03 in mode 8 and minimum damping factor were found in mode 1 to mode 4, 7 and also damping factor was found 0.02 in mode 5 and mode 6 respectively.

D. Surface crack at 40° with longitudinal axis

A typical plot of experimental results is shown in **Error! Reference source not found.**

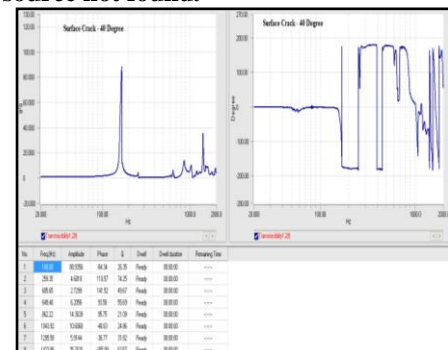


Fig. 17. Experimental results for surface crack at 40° for CCF

The Fig. 17 shows different magnitude of amplitude, modal frequencies and phase angle at resonance. All the details regarding resonance frequencies, amplitude at resonance, phase angle and Q-factor are also tabulated in Fig. 17.

The data of amplitude dependency on excitation frequencies are extracted from the Fig. 17. These data is used for drawing Fig. 18 which shows information inclusively on dependency of Amplitude with exciting frequency.

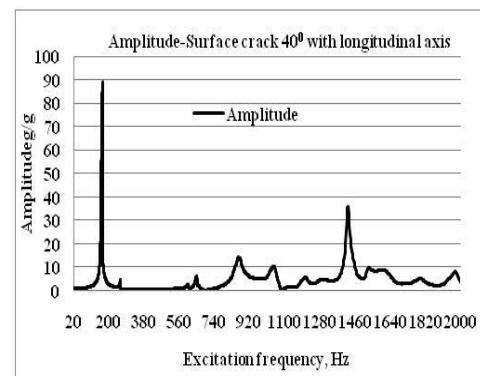


Fig. 18. Dependency of amplitude with excitation frequency for surface crack at 40°

The data of phase angle dependency on excitation frequencies are extracted from the Fig. 17 and drawn a new figure shown in Fig. 19 for the detailed information on phase angle of vibration.

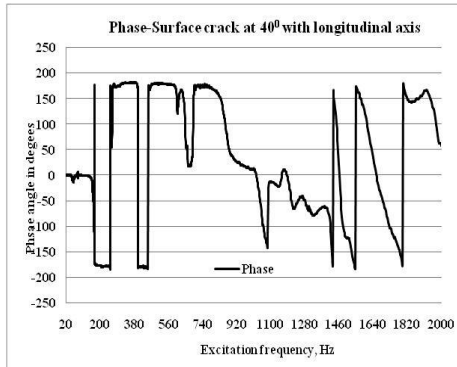


Fig. 19. Dependency of phase with Excitation frequency for surface crack at 40°

The experimental data of table in Fig. 17 are rounded off to nearest number. The amplitude is rounded up to full digit, phase angle rounded up to full number. The frequencies are rounded up to full number and Q-factor rounded up to full number. The rounded off data of frequencies, amplitudes, phase and Q-factors are tabulated and shown in **Error! Reference source not found.**. The damping factor (ξ) was estimated using formula: $\xi=1/2Q$. The estimated damping factors (ξ) are tabulated in **Error! Reference source not found.**.

TABLE V. AMPLITUDE, MODAL FREQUENCY, PHASE AND Q-FACTOR FOR SURFACE CRACK AT 40°

Surface crack at 40°					
Mode No.	Amplitude (g/g)	Modal Freq.(Hz)	Phase ($^\circ$)	Q-Factor	Damping factor (ξ)
1	89	168	-84	26.35	0.02
2	5	259	111	74.25	0.01
3	3	606	142	49.67	0.01
4	6	649	94	55.69	0.01
5	14	862	96	21.09	0.02
6	11	1044	-49	24.86	0.02
7	6	1206	-37	31.82	0.02
8	36	1424	-156	63.57	0.01

The **Error! Reference source not found.** shows highest magnitude of amplitude 89g/g at resonance frequency was found in first mode which is 168 Hz. Other lesser magnitude of amplitude was found 14, 11 and 36 g/g at the resonance frequencies of 862, 1044 and 1424 Hz in mode 5, 6 and 8 respectively. The other minimum magnitude of amplitude was found 5, 3, 6 and 6g/g at the resonance frequencies 259, 606, 649 and 1206 Hz in modes 2, 3, 4 and 7 respectively.

The **Error! Reference source not found.** shows the phase angles at the resonance modes. The phase angles at the resonance modes were found to be 111, 142, 94 and 96 at the modes 2, 3, 4 and 5 respectively. The response during these modes is lagging to forcing disturbance. The lagging found to be maximum in mode 3 and minimum in mode 4. The mode angles were found to be -84, -49, -37 and -156 $^\circ$ at the modes 1, 6, 7 and 8 respectively. The response of the system during

negative phase angle represents the leading of the system with respect to disturbing force. The leading was found to be highest in mode 7 and leading of the system gets reduced in modes 1, 4, 5, 6 and 8.

The **Error! Reference source not found.** shows damping factor (ξ) varies from 0.01 to 0.02. The maximum damping factor was found 0.02 in mode1, 5, 6 and 7 and minimum damping factor were found in mode 2, 3, 4 and 8 respectively.

E. Surface crack at 60° with longitudinal axis

A typical plot of experimental results is shown in Fig. 20.

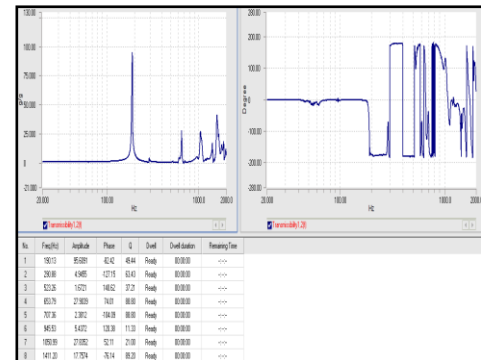


Fig. 20. Experimental results for surface crack at 60° for CCF boundary

The Fig. 20 shows different magnitude of amplitude, modal frequencies and phase angle at resonance. All the details regarding resonance frequencies, amplitude at resonance, phase angle and Q-factors are also shown in Fig. 20.

The data of amplitude dependency on excitation frequencies are extracted from the Fig. 20. These data is used for drawing Fig. 21 which shows information inclusively on dependency of amplitude with exciting frequency.

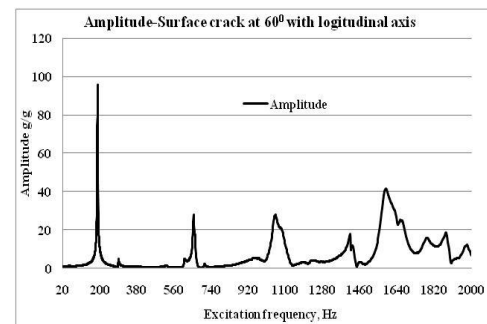


Fig. 21. dependency of amplitude with excitation frequency for surface crack at 60°

The data of phase angle dependency on excitation frequencies are extracted from the Fig. 20 and drawn a new figure shown in Fig. 22 for the detailed information on phase angle of vibration.

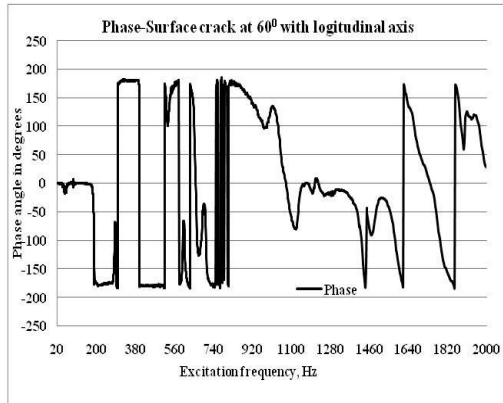


Fig. 22. Dependency of phase angles with excitation frequency for surface crack at 60°

The experimental data of table in Fig. 20 are rounded off to nearest number. The amplitude is rounded up to first full number, phase angle rounded up to full number. The frequencies are rounded up to full number and Q-factor rounded up to full number. The rounded off data of frequencies, amplitudes, phase and Q-factors are tabulated and shown in **Error! Reference source not found.**. The damping factor (ξ) was estimated using formula: $\xi=1/2Q$. The estimated damping factors (ξ) are tabulated in **Error! Reference source not found.**

The **Error! Reference source not found.** highest magnitude of amplitude 95.6g/g at resonance frequency was found in first mode which is 190 Hz. Other lesser magnitude of amplitude was found 27.9, 27.8 and 17.8 g/g at the resonance frequencies of 654, 1051 and 1411Hz in mode 4, 7 and 8 respectively. The other minimum magnitude of amplitude was found 4.9, 1.7, 2.4 and 5.4g/g at the resonance frequencies 291, 523, 707 and 946 Hz in modes 2, 3, 5 and 6 respectively

TABLE VI. AMPLITUDE, MODAL FREQUENCY, PHASE AND Q-FACTOR FOR SURFACE CRACK AT 60°

Mode No.	Amplitude (g/g)	Modal Freq.(Hz)	Phase (°)	Q-Factor	Damping factor
1	96	190	-82	49	0.01
2	5	291	-127	63	0.01
3	2	523	141	37	0.01
4	28	654	74	89	0.01
5	2	707	-104	89	0.01
6	5	946	120	11	0.04
7	28	1051	52	21	0.02
8	18	1411	-76	89	0.01

The **Error! Reference source not found.** shows the phase angles at the resonance modes. The phase angles at the resonance modes were found to be 141, 74, 94, 120 and 52 at the modes 3, 4, 6 and 7 respectively. The response during these modes is lagging to forcing disturbance. The lagging found to be maximum in mode 6 and minimum in mode 7. The mode angles were found to be -82, -127, -104 and -76° at the modes 1, 2, 5 and 8 respectively. The response of the system during negative phase angle represents the leading of the system with respect to disturbing force. The leading was found to be highest in mode 2 and leading of the system gets reduced in modes 1, 5 and 8.

The **Error! Reference source not found.** shows damping factor (ξ) varies from 0.01 to 0.04. The maximum damping

factor was found 0.04 in mode 6 and minimum damping factor was found 0.01 in mode 1, 2, 3, 4 and 5 respectively and also damping factor 0.02 found minimum in mode 7.

F. Surface crack at 80° with longitudinal axis

A typical plot of experimental results is shown in Fig. 23.



Fig. 23. Experimental results for surface crack at 80° for CCFF boundary conditions

The Fig. 23 shows different magnitude of amplitude, modal frequencies and phase angle at resonance. All the details regarding resonance frequencies, amplitude at resonance, phase angle and Q-factor are also tabulated in Fig. 23.

The data of amplitude dependency on excitation frequencies are extracted from the Fig. 23. These data is used for Fig. 24 which shows information inclusively on dependency of amplitude with exciting frequency.

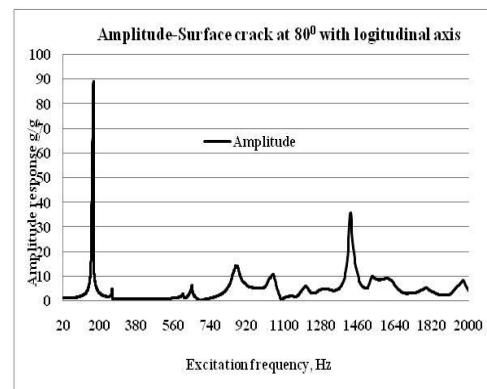


Fig. 24. Dependency of amplitude with excitation frequency for surface crack at 80°

The data of phase angle dependency on excitation frequencies are extracted from the Fig. 23 and drawn a new figure shown in Fig. 25 for the detailed information on phase angle of vibration.

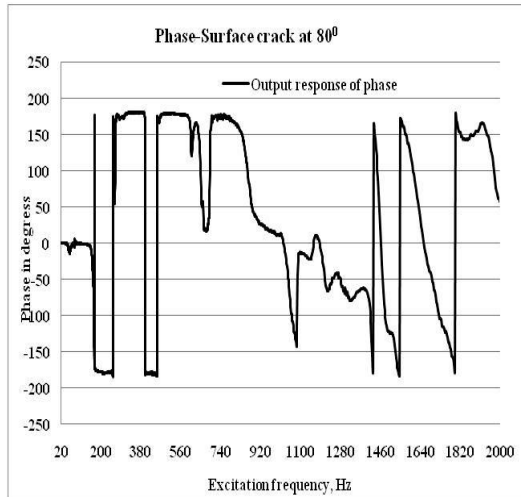


Fig. 25. Dependency of phase angles with excitation frequency for surface crack at 80°

The experimental data of table in Fig. 23 are rounded off to nearest full number. The amplitude is rounded up to first number, phase angle rounded up to full number. The frequencies are rounded up to full number and Q-factor rounded up to full number. The rounded off data of frequencies, amplitudes, phase and Q-factors are tabulated and shown in **Error! Reference source not found.** The damping factor (ξ) was estimated using formula: $\xi=1/2Q$. The estimated damping factors (ξ) are tabulated in **Error! Reference source not found.**

TABLE VII. : AMPLITUDE, MODAL FREQUENCY, PHASE AND Q-FACTOR FOR SURFACE CRACK AT 80°

Mode No.	Amplitude (g/g)	Modal Freq.(Hz)	Phase (°)	Q-Factor	Damping Factor (ξ)
1	89	168	-84	26	0.02
2	5	259	111	74	0.01
3	3	606	142	50	0.01
4	6	649	94	56	0.01
5	14	862	96	21	0.02
6	11	1044	-49	25	0.02
7	6	1206	-37	32	0.02
8	36	1424	-156	64	0.01

The **Error! Reference source not found.** shows highest magnitude of amplitude 89g/g at resonance frequency was found in first mode which is 168 Hz. Other lesser magnitude of amplitude was found 14, 10 and 36 g/g at the resonance frequencies of 862, 1044 and 1424Hz in mode 5, 6 and 8 respectively. The other minimum magnitude of amplitude was found 5, 3, 6 and 6 g/g at the resonance frequencies 259, 606, 649 and 1206 Hz in modes 2, 3, 4 and 7 respectively.

The **Error! Reference source not found.** shows the phase angles at the resonance modes. The phase angles at the resonance modes were found to be 111, 142, 94 and 96° at the modes 2, 3, 4 and 5 respectively. The response during these modes is lagging to forcing disturbance. The lagging found to be maximum in mode 3 and minimum in mode 4. The mode angles were found to be -84, -49, -37 and -156° at the modes 1, 6, 7 and 8 respectively. The response of the system during negative phase angle represents the leading of the system with respect to disturbing force. The leading was found to be

highest in mode 8 and leading of the system gets reduced in modes 1 and 2.

The **Error! Reference source not found.** shows damping factors (ξ) varies from 0.01 to 0.02. The maximum damping factor was found 0.04 in mode 1, 5, 6 and 7 and minimum damping factor was found 0.01 in mode 2, 3, 4 and 8 respectively.

G. Surface crack at 90° with longitudinal axis

A typical plot of experimental results is shown in Fig. 26

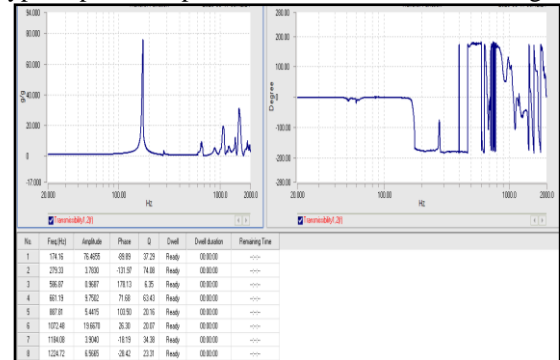


Fig. 26. Experimental results for surface crack at 90° for CCF

The Fig. 26 shows different magnitude of amplitude, modal frequencies and phase angle at resonance. All the details regarding resonance frequencies, amplitude at resonance, phase angle and Q-coefficients are also tabulated in Fig. 26.

The data of amplitude dependency on excitation frequencies are extracted from the Fig. 26. These data is used for drawing Fig. 27 which shows information inclusively on dependency of Amplitude with exciting frequency.

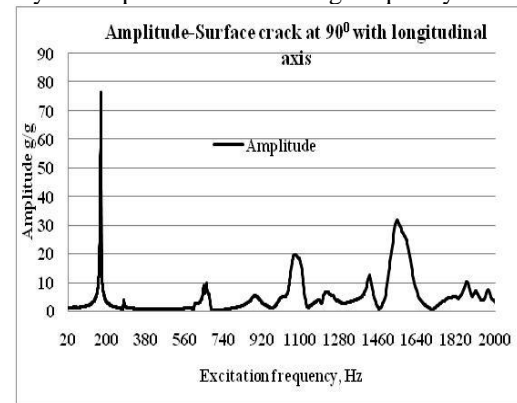


Fig. 27. Dependency of amplitude with excitation frequency for surface crack at 90°

The data of phase angle dependency on excitation frequencies are extracted from the Fig. 26 and drawn a new figure shown in Fig. 28 for the detailed information on phase angle of vibration.

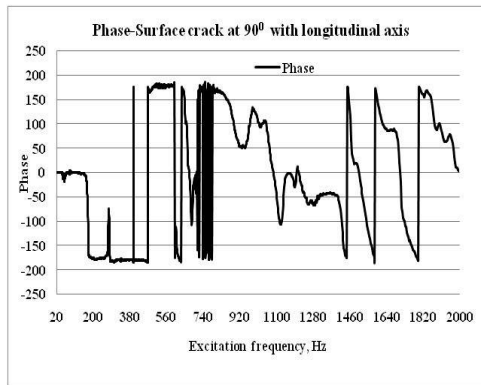


Fig. 28. Dependency of phase on excitation frequency for surface crack at 90°

The experimental data of table in Fig. 26 are rounded off to full number. The amplitude is rounded up to full number, phase angle rounded up to full number. The frequencies are rounded up to full number and Q-coefficient rounded up to full number. The rounded off data of frequencies, amplitudes, phase and Q-coefficients are tabulated and shown in **Error! Reference source not found.** The damping coefficient (ξ) was estimated using formula: $\xi=1/2Q$. The estimated damping factors (ξ) are tabulated in **Error! Reference source not found.**

TABLE VIII. AMPLITUDE, MODAL FREQUENCY, PHASE AND Q-COEFFICIENT FOR SURFACE CRACK AT 90°

Surface crack at 90° with longitudinal axis					
Mode No.	Amplitude (g/g)	Modal Freq. (Hz)	Phase (°)	Q-Coefficient	Damping coefficient (ξ)
1	77	174	-90	37	0.01
2	4	279	-132	74	0.01
3	1	587	178	6	0.08
4	9	661	72	63	0.01
5	5	888	104	20	0.02
6	20	1072	26	20	0.02
7	4	1184	-18	34	0.01
8	7	1225	-28	23	0.02

H. Estimated average magnitude of amplitudes

The **Error! Reference source not found.** shows estimated average values of magnitude of amplitude from the three different trials for different modes of solid plates and plates with surface cracks oriented in different direction with longitudinal axis of the plates are tabulated in **Error! Reference source not found.**

TABLE IX. AVERAGE AMPLITUDE RESPONSE OF SOLID & ARBITRARY ORIENTED SURFACE CRACKS

Average Amplitude (g/g)							
Mode No	Solid plate	Surface cracks					
	-	0°	20°	40°	60°	80°	90°
1	92	96	72	52	98	74	77
2	1	3	3	3	3	3	2
3	4	8	1	13	6	2	1
4	34	15	2	13	15	20	4
5	4	16	12	10	1	6	22
6	2	2	10	5	3	5	7
7	10	9	8	3	12	4	2
8	5	18	1	3	7	14	5

The average magnitudes amplitudes tabulated in **Error! Reference source not found.** are used for drawing bar chart and shown in Fig. 29.

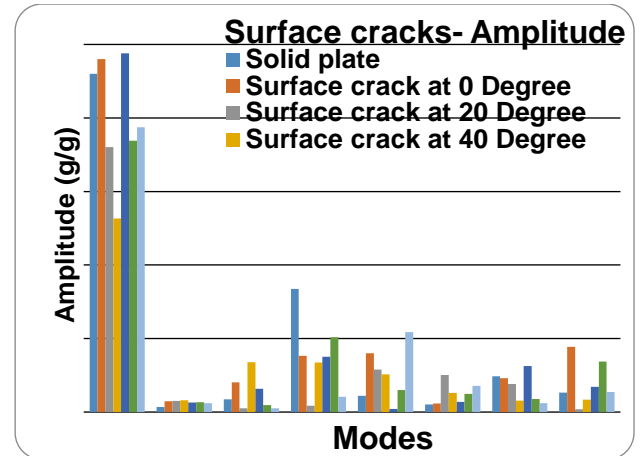


Fig. 29. Average magnitude of amplitude with modal number of solid & arbitrary oriented surface cracks

The average values magnitude of amplitudes in model for solid plate and plate with surface cracks oriented differently with longitudinal axis of the rectangular plate lies between 92 and 52 g/g. The average magnitude of amplitude in mode 4 for solid plate and plate with surface crack oriented differently with longitudinal axis of the plate lies 34 and 2 g/g. The average value magnitude of amplitudes in mode 2, 3, 5, 6, 7, 8 for solid plate and plate with surface cracks oriented differently with longitudinal axis of the rectangular plate lies between 22 and 1.

In general the fluctuations in magnitude of average amplitudes of vibration of solid plate and plate with surface cracks oriented differently with longitudinal axis of the rectangular plate fluctuates larger extent in model and mode 4. The extent of fluctuation, the magnitude of average amplitude in mode2, 3, 5, 6, 7 and 8 is found to be narrow down compared to the model and mode 4.

The presence of surface crack and its orientation with respect longitudinal axis was found to alter the amplitude of vibration in first mode compared to solid plate. The magnitudes of amplitude in first mode for surface cracked plate were found to be less than solid plate except for 0° and 60° oriented surface crack. This could be attributed to alter the potential energy of the plate due to surface crack. Such generalization not found at higher modes

I. Estimated average magnitude of amplitude

The **Error! Reference source not found.** shows estimated average values of magnitude of amplitude from the three different trials for different modes of solid plates and plates with surface cracks oriented in different direction with longitudinal axis of the plates are tabulated in **Error! Reference source not found.**

TABLE X. AVERAGE MODAL FREQUENCIES OF SOLID & ARBITRARY ORIENTED SURFACE CRACKS

Average Modal frequency							
Mode No	Solid plate	Surface cracks					
	-	0°	20°	40°	60°	80°	90°
1	188	183	175	169	191	170	176
2	303	282	397	390	313	281	281
3	504	460	436	432	606	535	412
4	651	649	554	707	670	647	558
5	696	819	733	800	724	741	720
6	835	894	807	929	847	869	816
7	1004	1013	938	1011	1056	1023	926

8	1110	1319	1025	1114	1247	1145	1058
---	------	------	------	------	------	------	------

The average magnitudes of modal frequencies tabulated in **Error! Reference source not found.** are used for drawing bar chart and shown in Fig. 30.

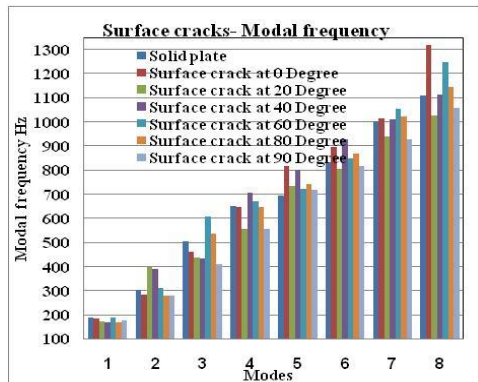


Fig. 30. Average magnitude of modal frequency of solid & arbitrary oriented surface cracks

The average values magnitude of modal frequencies in mode1 for solid plate and plate with surface cracks oriented differently with longitudinal axis of the rectangular plate in the range 169 and 191Hz. The average values magnitude of modal frequencies in mode2 for solid plate and plate with surface cracks oriented differently with longitudinal axis of the rectangular plate in the range 281 and 390Hz. The average values magnitude of modal frequencies in mode3 for solid plate and plate with surface cracks oriented differently with longitudinal axis of the rectangular plate in the range 412 and 606Hz. The average values magnitude of modal frequencies in mode4 for solid plate and plate with surface cracks oriented differently with longitudinal axis of the rectangular plate in the range 554 and 707Hz. The average values magnitude of modal frequencies in mode5 for solid plate and plate with surface cracks oriented differently with longitudinal axis of the rectangular plate in the range 554 and 707Hz. The average values magnitude of modal frequencies in mode6 for solid plate and plate with surface cracks oriented differently with longitudinal axis of the rectangular plate in the range 807 and 869Hz. The average values magnitude of modal frequencies in mode7 for solid plate and plate with surface cracks oriented differently with longitudinal axis of the rectangular plate in the range 926 and 1056Hz. The average values magnitude of modal frequencies in mode8 for solid plate and plate with surface cracks oriented differently with longitudinal axis of the rectangular plate in the range 1025 and 1319Hz respectively.

The modal frequencies in general increased with mode numbers irrespective of surface crack its orientation. This could be attributed to storing the potential energy due to mode configuration.

J. Estimated average magnitude of Phase angle

The **Error! Reference source not found.** shows estimated average values of magnitude amplitude from the three different trials for different modes of solid plates and plates with surface cracks oriented in different direction with longitudinal axis of the plates are tabulated in **Error! Reference source not found.**

TABLE XI. AVERAGE PHASE ANGLE OF SOLID & ARBITRARY ORIENTED SURFACE CRACKS

Mode No	Average phase angles						
	Solid plate	Surface cracks					
	-	0°	20°	40°	60°	80°	90°
1	-87	-85	-114	-91	-87	-90	-95
2	-56	49	-59	-61	-154	-75	132
3	39	27	-69	-92	123	-35	-165
4	5	-11	-46	88	49	89	138
5	-93	-13	80	-64	59	-8	65
6	111	-23	-49	112	125	59	-88
7	112	-31	21	100	77	53	112
8	32	-52	39	31	14	0	74

The average magnitudes of modal frequencies tabulated in **Error! Reference source not found.** are used for drawing bar chart and shown in Fig. 31.

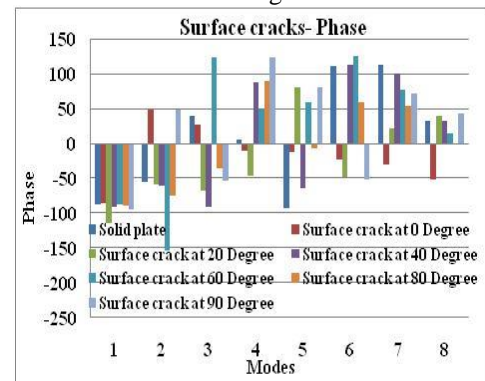


Fig. 31. : Average magnitude of phase angles of solid & arbitrary oriented surface cracks

The average values magnitude of phase angles in mode1 for solid plate and plate with surface cracks oriented differently with longitudinal axis of the rectangular plate lies between -85 and -90°. The average magnitude of amplitude in mode 4 for solid plate and plate with surface crack oriented differently with longitudinal axis of the plate lies 5 and 138°. The average value magnitude of amplitudes in mode 2, 3, 5, 6, 7, 8 for solid plate and plate with surface cracks oriented differently with longitudinal axis of the rectangular plate lies between 0 and -165°.

The system irrespective orientation of surface crack was found to lagging in first mode. The phase angle was found to be positive and negative in higher modes. Such behavior also could be attributed to storage of potential energy due to configuration of the plate.

K. Estimated average magnitude of damping factor

The **Error! Reference source not found.** shows estimated average values of magnitude damping coefficient from the three different trials for different modes of solid plates and plates with surface cracks oriented in different direction with longitudinal axis of the plates are tabulated in **Error! Reference source not found.**

TABLE XII. AVERAGE MAGNITUDE OF DAMPING COEFFICIENT OF SOLID & ARBITRARY ORIENTED SURFACE CRACKS

Mode No	Average Damping coefficient						
	Solid plate	Surface crack					
	-	0°	20°	40°	60°	80°	90°
1	0.01	0.01	0.01	0.02	0.01	0.01	0.01
2	0.04	0.01	0.01	0.01	0.02	0.02	0.01
3	0.01	0.01	0.02	0.01	0.01	0.01	0.04
4	0.01	0.01	0.01	0.02	0.01	0.01	0.02
5	0.01	0.01	0.01	0.01	0.01	0.01	0.01

6	0.02	0.01	0.01	0.01	0.02	0.01	0.01
7	0.01	0.01	0.01	0.01	0.02	0.04	0.01
8	0.03	0.04	0.03	0.04	0.01	0.02	0.03

The average magnitudes of damping coefficient in different modes of vibration are used for drawing bar and shown in TABLE XII. .

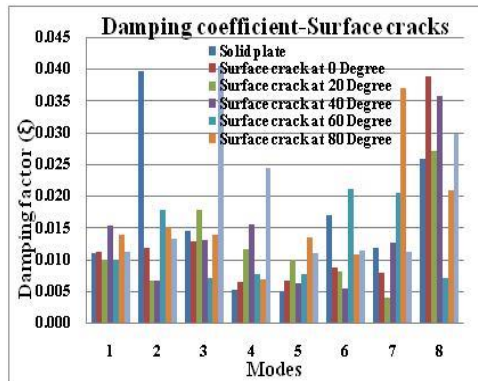


Fig. 32. Average magnitude of damping coefficient of solid & arbitrary oriented surface cracks

The average values magnitude damping factor in model for solid plate and plate with surface cracks oriented differently with longitudinal axis of the rectangular plate lies between 0.01 and 0.02. The average magnitude of amplitude in mode 4 for solid plate and plate with surface crack oriented differently with longitudinal axis of the plate lies 0.01 and 0.02. The average value magnitude of amplitudes in mode 2, 3, 5, 6, 7, 8 for solid plate and plate with surface cracks oriented differently with longitudinal axis of the rectangular plate lies between 0.01 and 0.04.

The damping coefficient found to be in the order of 0.01 except in the case of in mode 2 of solid plate and surface crack with arbitrary oriented 90° in mode 3 and surface crack with arbitrary oriented 40° in mode 4 and surface crack with arbitrary oriented 40° and 90° in mode 4 and surface crack with arbitrary oriented 60° in mode 6 and surface crack with arbitrary oriented 80° in mode 7 and surface crack with arbitrary oriented 0° and 40° in mode 3

IV. CONCLUSION

- ❖ The amplitude of vibration was found to be influenced by the surface cracks and its orientation with respect to longitudinal axis.
- ❖ The modal frequencies, irrespective of cracks and its orientations, in general increased with mode number.
- ❖ The system was found to be lagging in mode 1 and both lagging and leading in other modes,
- ❖ The redistribution of potential energy which depends on the mode configuration was found to be a factor influencing the dynamic response.

REFERENCE:

- [1] *Vibration analysis of plates with one free edge using energy method (CCCF plate)*. **Ibearughulem et al.** s.l.: International journal of engineering and technology, 2014, Vols. 4, No.1.
- [2] *Transverse vibration of the thin plates: frequency domain spectral element modeling and analysis*. **Ilwook et al.** s.l.: Mathematical problem in engineering, 2015, Vol. 2015.
- [3] *A simplified method for natural frequency analysis of multiple cracked beam*. **Lien, Khiem and.** s.l.: Journal of sound and vibration, 2001, Vols. 245(4),737-751.

- [4] *Free vibration analysis of isotropic and orthotropic clamped plates using energy approach*. **Naimi, Zarza and.** s.l.: Science and technology, 2004, Vols. 92-97.
- [5] *Analytical modeling and vibration analysis of partially cracked rectangular plates with different boundary conditions and loading*. **et al, Asif Israr.** Glasgow: journal of applied mechanics, 2009, Vols. 76/011005-1.
- [6] *Vibration analysis of rectangular plates with clamped corners*. **Obeidat, gharaibeh and.** s.l.: research article, 2018.
- [7] *Vibration analysis of stiff plate with cut out*. **Tushar Choudhary, Ashwinkumar.** 1, India: international journal of technical research and application, 2015, Vol. 3.
- [8] *Prediction of natural frequencies of vibration of rectangular plates with rectangular cutouts*. **Ali and Atwal.** 6, s.l.: computer and structures, 1980, Vols. 12, pp.819-823.
- [9] *Experimental determination of damping ratio at higher modes for use in modal superposition*. **Ramamurthy et al.** s.l.: journal of engineering and technology research, 2012, Vols. 4(6), pp.114-128.
- [10] *Vibration analysis of a rectangular thin plates with two parallel cracks*. **Lam, Yin and.** s.l.: Advanced in structural engineering, 2010, Vols. 13, No.4.
- [11] *Effects of crack on natural frequency*. **Gade et al.** India: international journal on theoretical and applied research in mechanical engineering, 2016, Vols. 5, No.1.
- [12] *Experimental study of free vibration of clamped rectangular plates with narrow slits*. **Ichinomia, Koichi Maruyama and Osamu.** s.l.: JSME international journal, 1989, Vols. 32, No.2.
- [13] *An approximate analytical procedure for natural vibration analysis of free rectangular plates*. **IVO Senjanovi, Marko tomic, Nikola Vladmir and Neven Hadzic.** Zagerab: Elsevier, 2015, Vols. 95, 101-114.
- [14] *Analytical modeling and vibration analysis of internally cracked rectangular plates*. **P.V. Joshi, N.K. Jain, G.D Ramtekar.** India: journal of sound and vibration, 2014, Vols. 333, 5851-5864.
- [15] *Experimental and numerical study of free vibration characteristics of plates*. **Rangith, Vishwas and.** 7, Mandya: international journal for research in applied science and technology, 2019, Vol. 7.